

The differential energy distribution of the universal density profile of dark halo

C. Hanyu and A. Habe

Division of Physics, Graduate School of Science, Hokkaido University, Sapporo 060-0810, Japan

chiaki@astro1.sci.hokudai.ac.jp

habe@astro1.sci.hokudai.ac.jp

ABSTRACT

We study the differential energy distribution of dark matter halos, carrying out cosmological N -body simulation. We give an analytical formula of the differential energy distribution of dark matter in the halos obtained by the numerical simulation. From the analytical formula we reconstruct the density profile described by the Navarro, Frenk, & White (NFW) profile. The NFW profile is consistent with the analytical formula of our fractional mass distribution. We find that a parameter in our analytical formula of differential energy distribution which is related with the slope of inner cusp of dark halo. We obtain the distribution function for the NFW profile which has sharp cut off at the high binding energy. We discuss physical reason of form of the analytical formula.

Subject headings: Cosmology: dark matter; Galaxies: Formation, Halos, clusters

1. Introduction

It is interesting to understand how the density profiles of galaxies and clusters of galaxies have formed. Navarro, Frenk and White (1995, 1996, 1997; NFW) have shown in their N -body simulations of Cold Dark Matter (CDM) in the standard biased CDM and four power law spectra with indices $n = 0, -0.5$, and -1 , open CDM ($\Omega_0 = 0.1$) with power-law spectra ($n = 0$ and -1), and Λ CDM cosmology that density profiles of dark halos have an universal profile described as

$$\rho(r) \propto \frac{1}{\left(\frac{r}{r_s}\right) \left(1 + \frac{r}{r_s}\right)^2}. \quad (1)$$

Several investigators have shown that the formula provides a good fit to their numerical results (Cole and Lacey 1996, Tormen, Bouchet & White 1997, Huss, Jain & Steinmetz 1999, Thomas *et al.* 1998). However, some other simulations (Fukushige & Makino 1997; Moore *et al.* 1998; Okamoto & Habe 1999, 2000) indicate that their density profiles have steeper inner cusp than the

NFW profile. Jing (2000) gives his numerical results that steeper cusps of density profile are found in recent mergers and in dark halos with substructures, by a large set of high resolution cosmological simulations.

Subramanian, Cen and Ostriker (2000) discussed the general theoretical grounds of the density profiles. They discussed that there is a possible connection between slope of inner region of dark halo and the formation epoch and proposed that there is possible relation to cosmological parameters.

However, physical reason of the NFW profile have not been explored, although it is very important to understand formation of galaxies and clusters of galaxies.

We study the differential energy distribution of the NFW profile, $dM/d\varepsilon$, where ε is the binding energy. The differential energy distribution was studied to understand virialization process of N -body system (van Albada 1982). Binney (1982) shows that $dM/d\varepsilon$ of the elliptical galaxies is approximated by the Boltzmann factor, if surface

brightness of elliptical galaxies obeys the de Vaucouleurs' $r^{1/4}$ law and their mass-to-light ratio is constant. It is interesting to study phase space structure of virialized objects with the NFW profile, since the differential energy distribution may give insight of the relaxation process (Binney & Tremaine 1987).

In this paper we calculate formation of clusters of galaxies by N -body simulation and we study the differential energy distribution of the clusters in our numerical results. We find an analytical formula of the fractional mass distribution that is defined by the differential distribution divided by mass of the object, is fitted by an analytical formula. We show that the NFW profile is consistent with our analytical formula of the fractional mass distribution. Using the iteration method, we construct the density profile from the analytical formula to show how the slope of the cusp of the density changes with parameters in our analytical formula.

In the next section, we illustrate our numerical method. In the section 3, we present our numerical results. We show the iteration method and give results by this method in the section 4, and we summarize and discuss our results in the section 5.

2. Numerical simulation

We use the Hofman and Ribak's (Hofman and Ribak 1991) procedure to set initial conditions in order to have a massive dark halo near the centre of a simulation box. The cosmology is SCDM model (e.g. Davis *et al.* 1985) ($\Omega = 1$, $\sigma_8 = 0.67$, $H_0 = 100h$ km s $^{-1}$ Mpc $^{-1}$, and $h = 0.5$).

Numerical simulations are carried out using GRAPESPH code. GRAPE is a special purpose hardware to calculate gravitation between N -body particles (Sugimoto *et al.* 1990). We combined Smoothed Particle Hydrodynamics (SPH) (Monaghan, 1992) with GRAPE. We select massive halos of which mass is as large as that of cluster of galaxies and calculate their density profile and the fractional mass distribution.

Mass of a CDM particle and a SPH particle are $5.89 \times 10^{11} M_\odot$ and $3.10 \times 10^{10} M_\odot$, respectively. Gravitational softening length is 100 kpc. Both number of CDM and SPH particles are 29855, respectively. Size of the simulation box is 80 Mpc.

3. Numerical results

3.1. Density distribution

Before we show our numerical results, we summarize the NFW profile. NFW proposed that the profile of the dark halo of cosmological object in their numerical results as

$$\frac{\rho(r)}{\rho_{cr}} = \frac{\delta_c}{\left(\frac{r}{r_s}\right) \left(1 + \left(\frac{r}{r_s}\right)\right)^2}, \quad (2)$$

where $r_s = r_{200}/c$, c is a dimensionless parameter and $\rho_{cr} = (3H_0^2)/(8\pi G)$ is the critical density of the universe. Since the mass of the halo is $M(r_{200}) = 200 \times 4\pi/3 \rho_{cr} r_{200}^3$, there is a relation between δ_c and c as

$$\delta_c = \frac{200}{3} \frac{c^3}{[\ln(1+c) - c/(1+c)]}, \quad (3)$$

where $M(r_{200})$ is the mass of which averaged density inside r_{200} is 200 times ρ_{cr} .

This density profile has a cusp in the inner region, $\rho(r) \propto r^{-1}$. $\rho(r) \propto r^{-3}$ in the outer region. NFW97 showed that the parameter c decreases with halo mass.

Table 1 is physical values of our simulated clusters. The units of mass, and X-ray temperature are $10^{15} M_\odot$ and 10^8 K, respectively.

Figure 1 shows a density profile of our simulated typical rich cluster, CLc, and the NFW profile with $c = 4.4$ which fits well the numerical result. Density profiles of dark halos obtained by us agree well with the NFW profile in the range from the gravitational softening length to r_{200} .

3.2. The differential energy distribution

We introduce the differential energy distribution, $dM/d\varepsilon$ which gives the mass of dark matter in the dark halo with binding energy between ε and $\varepsilon + d\varepsilon$, where ε is the specific binding energy,

$$\varepsilon = \Psi(r) - \frac{1}{2}v^2, \quad (4)$$

and a relative potential, $\Psi \equiv -\Phi + \Phi_0$. Φ is gravitational potential and we choose Φ_0 to be such that a distribution function, f , is $f > 0$ for $\varepsilon > 0$ and $f = 0$ for $\varepsilon \leq 0$. In our analysis, ε is normalized by GM_{200}/r_{200} . And we also introduce the

fractional mass distribution as the differential energy distribution divided by the total mass of the dark halo, $N(\varepsilon) = dM/d\varepsilon/M$.

Figure 2 shows the fractional mass distribution of CLC. In figure 2, we also show $N(\varepsilon)$ given by

$$N(\varepsilon) = N_0 \left[1 - (1 - q) \left(\frac{\varepsilon}{\varepsilon_0} \right) \right]^{q/(1-q)}, \quad (5)$$

with $q = 0.667$ and $\varepsilon_0 = 1.47$. Figure 2 shows that equation (5) agrees well with our numerical results in the range of $0.5 < \varepsilon < 4$. There is cut off near $\varepsilon \simeq 4$. We find the fractional distribution $N(\varepsilon)$ can be fitted by following formula, for $q \simeq 0.6-0.7$ and $\varepsilon_0 \simeq 1.2 - 1.5GM_{200}/r_{200}$ for rich clusters in our numerical results.

In table 2 we give N_0 , q , and ε_0 of our numerical results for rich clusters.

We have shown from our N - body simulation that the fractional mass distribution is also well fitted by the equation (5). However, near $\varepsilon = 4$ in figure 2 there are small number of N -body particles. We should confirm consistency between $N(\varepsilon)$ given by equation (5) and the NFW profile. We give a fractional mass distribution from the NFW profile as follows for the comparison.

We assume that phase-space distribution function $f(\mathbf{x}, \mathbf{v})$ depends ε . At a radius r , velocity of a dark matter particle of the binding energy, ε , is $v = \sqrt{2(\Psi - \varepsilon)}$. The density profile may be given as follows (Binney and Tremaine 1987)

$$\rho(r) = 4\pi \int_{\Psi(r_g)}^{\Psi(r)} f(\varepsilon) [2(\Psi - \varepsilon)]^{1/2} d\varepsilon, \quad (6)$$

where r_g is the edge of the dark halo. From this equation, we may give $f(\varepsilon)$ as

$$f(\varepsilon) = \frac{1}{\sqrt{8}\pi^2} \frac{d}{d\varepsilon} \int_{\varepsilon_{min}}^{\varepsilon} \frac{d\rho/d\Psi}{[\varepsilon - \Psi]^{1/2}} d\Psi, \quad (7)$$

where $\varepsilon_{min} = \Psi(r_g)$.

Equation (6) gives mass M as

$$M(r) = 16\pi^2 \int_0^r r'^2 dr' \times \int_0^{\Psi(r)} f(\varepsilon) [2(\Psi - \varepsilon)]^{1/2} d\varepsilon. \quad (8)$$

From equation (8), the differential energy distribution is

$$\frac{dM(\varepsilon)}{d\varepsilon} = f(\varepsilon)g(\varepsilon), \quad (9)$$

where

$$g(\varepsilon) = 16\pi^2 \int_0^{r_m(\varepsilon)} [2(\Psi - \varepsilon)]^{1/2} r'^2 dr', \quad (10)$$

and $r_m(\varepsilon)$ is maximum radius that can reached by a particle of the binding energy ε .

If we assume the density profile is the NFW profile, we get $dM/d\varepsilon$ from the equations (7), (9), and (10) for the NFW profile.

Figure 3 shows the fractional mass distribution of NFW obtained in this way and $N(\varepsilon)$ given by equation (5). We show that $N(\varepsilon)$ given by equation (5) is consistent with the NFW profile. We note that the cut off at high binding energy seen in figure 2 is not artifact due to limitation of our numerical resolutions.

Figure 4 shows the distribution function of the NFW profile obtained by the above method. Since lower binding energy particles evaporate from the dark halo, their fraction become small. This form of function is similar to the distribution function of King model, $f_K(\varepsilon) \propto (e^{\varepsilon/\sigma^2} - 1)$ (Binney 1982). On the other hand, there is a peak and sharp cut off at the high binding energy. This part corresponds to the central cusp. Although the distribution function of NFW profile have cut off at the high energy, the distribution function of King model does not have such cut off. This is an important difference between them.

4. The fractional mass distribution, density profile, and the distribution function

We find that the NFW profile satisfies the fractional mass distribution given by equation (5) with $q \simeq 0.6 - 0.7$. We study how the density profile changes when we change the parameter q and ε_0 in equation (5). In this study, we use an iteration method as shown in the next subsections.

4.1. The iteration method

Binney (1982, and see also Binney and Tremaine 1987) studied the phase space structure of galaxies of which surface brightness is the de Vaucouleurs' $r^{1/4}$ law. We apply his method to our study of the phase space structure of dark halo with the NFW profile. We obtain the density profile and the phase space distribution which are consistent

with equation (5), using the iteration method. The procedure is as follows.

We assume the dark halo is spherically symmetric. From equation (5), we assume $dM(\varepsilon)/d\varepsilon$ given by equation,

$$\frac{dM(\varepsilon)}{d\varepsilon} = M_0 \left[1 - (1 - q) \left(\frac{\varepsilon}{\varepsilon_0} \right) \right]^{q/(1-q)}, \quad (11)$$

where $M_0 = 1.0$. We use a trial function of a density profile, to calculate a gravitational potential in $g_0(\varepsilon)$,

$$\rho_0(x) = \frac{\rho_c}{\left(1 + \left(\frac{x}{x_c} \right)^2 \right)^{3/2}}, \quad (12)$$

where $x_c = r_c/r_{200} = 0.1$. This trial function is similar to the β -model of X-ray surface brightness of clusters of galaxies. We obtain relative potential from this trial density function. The relative potential is written as

$$\begin{aligned} \Psi(x) = & 4\pi G \left[\frac{1}{x} \int_0^x \rho_0(x') x'^2 dx' \right. \\ & \left. + \int_x^{x_o} \rho_0(x') x' dx' \right] + \Phi_{x_o}, \quad (13) \end{aligned}$$

where $x = r/r_{200}$, and $x_o = 10$ is assumed. Φ_{x_o} is chosen to be $f > 0$ for $\varepsilon > 0$ and $f = 0$ for $\varepsilon \leq 0$. We obtain $g_0(\varepsilon)$ by equation (10) for ρ_0 . From equation (9),

$$f_0(\varepsilon) = \frac{dM(\varepsilon)/d\varepsilon}{g_0(\varepsilon)}. \quad (14)$$

Next, we calculate new density as,

$$\begin{aligned} \rho_{i+1}(x) = & (1 - \alpha)\rho_i(x) \\ & + \alpha \times 4\pi \int_{\Psi_i > \varepsilon} f_i(\varepsilon) \sqrt{2(\Psi_i - \varepsilon)} d\varepsilon, \quad (15) \end{aligned}$$

where i is an iterative index and α is an arbitrary constant of convergence. Here we assume $\alpha = 0.5$. Next we again follow the step from equation (13) to equation (15) by using ρ_1 instead of ρ_0 and we obtain ρ_2 . We continue until ρ_i becomes converge. In this way, we obtain ρ and $f(\varepsilon)$ which are consistent with equation (11).

4.2. The density profile and the distribution function

Using the Binney's iteration method, we reconstruct mass density profile from equation (11).

We show our result for $q = 0.67$ and $\varepsilon = 1.4$ in figure 5. A solid line is given by the iteration method and a dashed line is the NFW profile. We confirm that $dM(\varepsilon)/d\varepsilon$ characterizes well the NFW profile.

In figure 6, we show density profiles for different q but $\varepsilon = 1.4$. Smaller q (e.g. $q = 0.5$) results in shallower core in the inner region. On the other hand, larger q ($q > 0.67$) makes a cusp steeper than the NFW profile, density profile approaches $\rho \propto r^{-2}$ in the inner part, for $q \rightarrow 1$.

For various values of ε_0 , the density profiles are similar to the NFW for $q = 0.6$ as shown in figure 7. Absolute value of the density depends on ε_0 . Therefore, the slope of the cusp depends on only q , not ε_0 .

Figure 8 shows the distribution function, f , obtained by the iteration method for various values of q . These curves show the same dependence on ε in $0 < \varepsilon < 1$. Peak values of f are different each other. We also show the Boltzmannian distribution for comparison in figure 8. For large q , peak value of $f(\varepsilon)$ and the maximum binding energy of the distribution become large. We have shown that the density profile with large q have the steep cusp. Therefore, sharp peak of $f(\varepsilon)$ corresponds to the steep cusp.

Figure 9 shows f obtained by the iteration method for same q but various ε_0 . These curves do not show the same dependence on binding energy. Height of peaks of these curves is constant.

5. Summary and Discussion

We analyze the universal density profile of dark halo proposed by NFW and its differential energy distribution. Our main results are summarized as follows.

1. We study the fractional mass function $N(\varepsilon)$ for dark halo obtained by our numerical simulation and find its analytical formula which is the equation (5).
2. We show that the NFW profile is given by the equation (11).

3. We show that the slope of the cusp in the density profile changes with a value of the parameter q in the analytical formula.

We can regard that $N(\varepsilon)$ shows the statistical property of the NFW profile. If the NFW profile is universal, $q = 0.6 - 0.7$ in equation (5). Different q makes slope of a cusp different. Since q plays an important role, we should make clear what physical process determines q . Recent high resolution numerical simulation (Okamoto & Habe 1999, 2000) shows the steeper cusp, $\rho \propto r^{-1.5}$, than the the NFW profile. This profile corresponds to $q = 0.75 - 0.8$. Isothermal profile, $\rho \propto r^{-2}$, corresponds to $q = 1$.

We study $f(\varepsilon)$ for the NFW profile. The formula of this is not isothermal one nor the King formula $f_K \propto e^{\varepsilon/\sigma^2} - 1$. $f(\varepsilon)$ for the NFW profile have the energy cut off at the high end of ε . We should study the reason why $f(\varepsilon)$ has such a form. Lynden-Bell (1967) studied distribution function $f(\varepsilon)$ of a virialized system. Maximizing the Boltzmann entropy of the system, resulting distribution is isothermal profile, $\rho \propto r^{-2}$. In this case the system has infinite extend and infinite mass. This is not realistic for astronomical objects. Cosmological simulations have shown that galaxies and clusters of galaxies formed in these simulations have more rapid radial decline than isothermal in the outer part.

We note that the form of the distribution function relates with the cusp profile. For $q < 1$, there are the maximum binding energy ε_{\max} and the sharp peak in $f(\varepsilon)$ at ε_{\max} . Since there is ε_{\max} , phase space volume occupied by dark matter is limited than the isothermal profile. This may be the reason of the cusp profile different from $\rho \propto r^{-2}$. For $q < 1$, the distribution function $f(\varepsilon)$ changes with q values as shown in figure 8.

We note that the form of equations (5) and (11) are similar to the Tsallis' escort distribution,

$$\frac{P(E, T')}{P(0, T')} = \left[1 - (1 - q) \frac{E}{T'} \right]^{q/(1-q)}, \quad (16)$$

where T' is temperature parameter and q is entropic index (Tsallis, Mendes, & Plastino, 1998). Tsallis' non-extensive generalized statistics (Tsallis 1988) is paid attention in the area of statistics of a multi-fractal system. In non-extensive system (long-range microscopy memory, long range forces,

fractal space time) the following generalized entropy has been proposed :

$$S_q = k \frac{1 - \sum_i p_i^q}{q - 1} \quad \left(\sum_i p_i = 1; \quad q \in \mathbb{R} \right), \quad (17)$$

where k is a positive constant. Optimization of S_q yields, for the canonical ensemble,

$$p_i = Z_q^{-1} [1 - (1 - q)\varepsilon_i/T']^{1/(1-q)}, \quad (18)$$

$$Z_q \equiv \sum_i [1 - (1 - q)\varepsilon_i/T']^{1/(1-q)} \quad (19)$$

and, when $q \rightarrow 1$, the Boltzmann-Gibbs result is recovered. In this statistics an expected value of any physical variable is given by the Tsallis' escort distribution :

$$\langle A \rangle_q = \frac{\sum_i p_i^q A_i}{\sum_j p_j^q}, \quad (20)$$

where $\{A_i\}$ are the eigenvalues of an arbitrary observable A . The escort distribution, $P_i = p_i^q / \sum_j p_j^q$, is similar to the form of equation (5) and (11).

It is expected that long range interaction makes the system non-extensive. Our case may be the one of this cases. Our results suggests that differential energy distribution of collisionless particles is described by the escort distribution of the Tsallis statistics. This may indicate that energetic process of collisionless particles must be stochastic process.

In the Tsallis' escort distribution function, there is the maximum value of ε for $p_i > 0$ for $0 < q < 1$. This case is called superextensive. The shallower cusp profile in the the NFW profile shows the superextensive property of the dark matter distribution.

We show that the NFW profile corresponds to $q = 0.6 - 0.7$. Lavagno *et al.* (1998) have recently shown that fraction of peculiar velocity of cluster of galaxies (Bahcall & Oh 1996) is well explained by the Tsallis escort integral,

$$P(> v) = \frac{\int_v^{v_{max}} (1 - (1 - q)(v/v_0)^2)^{q/(1-q)} dv}{\int_0^{v_{max}} (1 - (1 - q)(v/v_0)^2)^{q/(1-q)} dv}. \quad (21)$$

They obtained $q = 0.23$ to fit the fraction of peculiar velocity of cluster of galaxies and is smaller than in our case. There is a conjecture that q

of system approaches unity when the system proceeds relaxation (Tsallis 1999). Our results in which $q = 0.6 - 0.7$ are consistent with this conjecture, since dark matter distribution in a cluster of galaxies is more relaxed system than the large scale motion of clusters of galaxies. The value of q must be related with the degree of relaxation of collisionless particles. $q = 1$ corresponds to isothermal distribution in the Tsallis statistics. The gravitational system like clusters of galaxies with the universal profile may be non-extensive because they formed recently.

We should study the reason why dark halo has the value of $q = 0.6 - 0.7$ in the hierarchical clustering scenarios. It is interesting to study the differential energy distribution of self-gravitational system formed in a circumstance without hierarchical clustering to make clear mechanism what determines q of the gravitational system.

We would like to thank Sumiyoshi Abe, Masayuki Fujimoto, and Seiichi Yachi for helpful comments and discussion.

REFERENCES

- Bahcall, N. A., & Oh., S. P., 1996, ApJ, 462, L49.
- Binney, J. 1982, MNRAS, 200, 951.
- Binney, J. & Tremain S., 1987, Galactic Dynamics (New Jersey : Princeton University Press).
- Cole, S. M., & Lacey, C., 1996, MNRAS, 281, 716.
- Davis, M., Efstathiou, G., Frenk, C.S., and White, S.D.M, 1985 ApJ, 292, 371
- Fukushige, T., & Makino, J., 1997, ApJ, 484, 40.
- Hofman, Y. & Ribak, E., 1991, ApJ, 380, L5.
- Huss, A., Jain, B., & Steinmetz, M, 1999, ApJ, 517, 64.
- Jing., Y. P., 2000, ApJ535, 30.
- Lavagno, A., Kaniadakis, G., Rego-Monteiro, M., Quarati., P., & Tsallis. C., 1998, Astro. Lett. and Communications, 35, 449.
- Lynden-Bell, D. 1967, MNRAS136, 101.
- Monaghan, J.J., 1992, ARRA, 30, 543
- Moore, B., Governato, F., Quinn, T., Stadel, J., & Lake, G., 1998, ApJ499, L5.
- Navarro, J. F., Frenk, C. S., & White S. D. M. 1995, MNRAS, 275, 720.
- Navarro, J. F., Frenk, C. S., & White S. D. M. 1996, ApJ, 462, 563.
- Navarro, J. F., Frenk, C. S., & White S. D. M. 1997, ApJ, 490, 493.
- Okamoto, T., & Habe, A. 1999, ApJ, 516, 591.
- Okamoto, T., & Habe, A. 2000, PASJ, 52, 457.
- Sugimoto, D., Chikada, Y., Makino, J., Ito, T., Ebisuzaki, T., & Umemura M., 1990, Nature, 345,33
- Subramanian, K., Cen, R., & Ostriker, J. P., 2000, ApJ, 538, 528,
- Thomas, P. A., *et al.*, 1998, MNRAS, 296, 1061.
- Tormen, G., Bouchet, F. R., & White, S. D. M., 1997, MNRAS, 286, 865.
- Tsallis, C., 1988, J. Stat. Phys. 52, 479.
- Tsallis, C., 1999, Braz. J. Phys. 29, 1.
- Tsallis, C., Mendes, R. S., Plastino, A. R., 1998, Physica A, 261, 534
- van Albada, T.S. 1982, MNRAS, 201, 939.

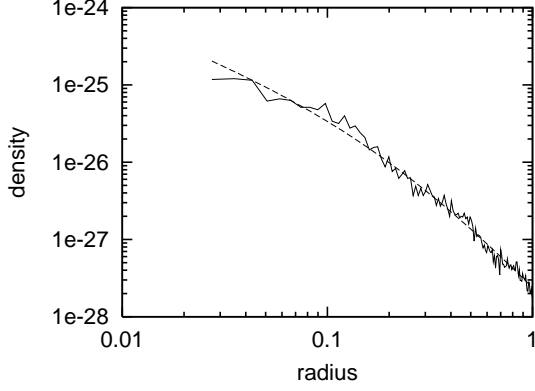


Fig. 1.— Density profile of one of simulated clusters, CLc, and the NFW profile with $c = 4.4$. Solid line is our numerical result and dashed line is the NFW profile. Radial distance is normalized by r_{200} . Our simulated clusters agree well with the NFW formula between the gravitational softening length to r_{200} .

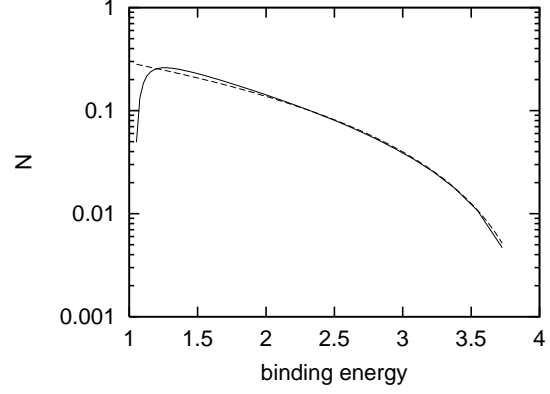


Fig. 3.— Fractional mass distribution of dark halo. Solid line is calculated by equations (7), (9), and (10) and dashed line is given by equation (5) with $q = 0.66$ and $\varepsilon_0 = 1.4$.

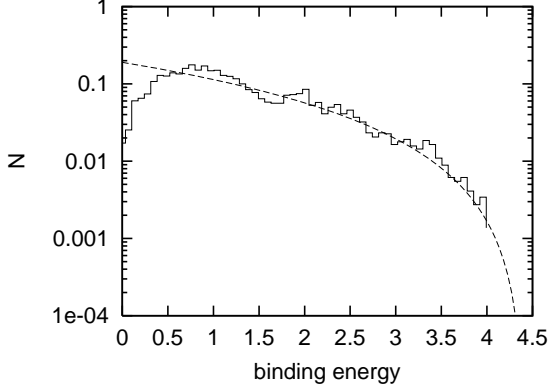


Fig. 2.— Fractional mass distribution of our simulated rich cluster, CLc. Solid line is our numerical result and dashed line is given by equation (5) with $q = 0.667$ and $\varepsilon_0 = 1.47$.

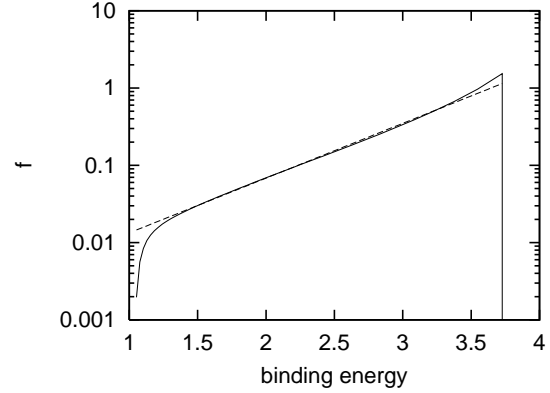


Fig. 4.— $f(\varepsilon)$ of the NFW profile. Solid line is $f(\varepsilon)$ and dashed line is a fitted exponential function.

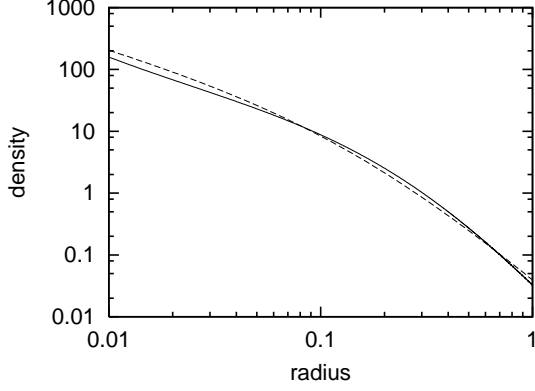


Fig. 5.— Density profile constructed by the iteration method, assuming the equation (11). Solid line is our result for $q = 0.67$ and $\varepsilon_0 = 1.4$ and dashed line is the NFW profile of $c = 6.59$. Radial distance is normalized by r_{200} .

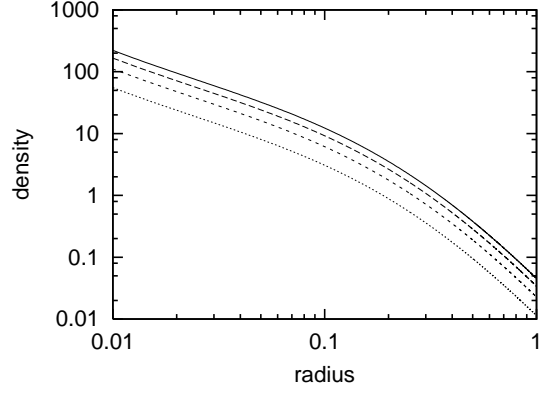


Fig. 7.— Density profiles for various ε . Dotted, short-dashed, dashed, and solid lines are for $\varepsilon_0 = 0.5, 1.0, 1.5$, and 2.0 , respectively. Density profiles are self-similar. However, their normalizations are different.

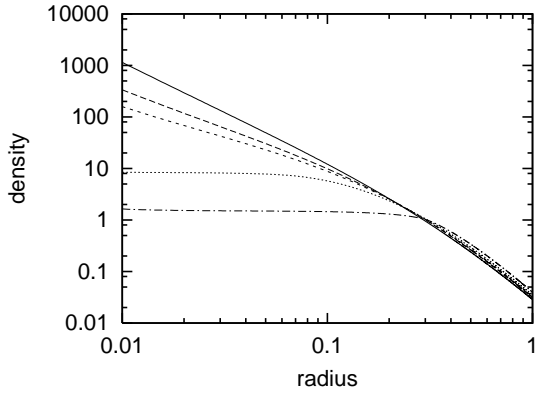


Fig. 6.— Density profiles for various q . Dot-dashed, dotted, short-dashed, dashed, and solid lines are for $q = 0.25, 0.5, 0.67, 0.75$, and 1.0 , respectively. Density profile with smaller q has a flat core. On the other hand, one approaches $\rho \propto r^{-2}$ in $r < 0.1$ for $q \rightarrow 1$.

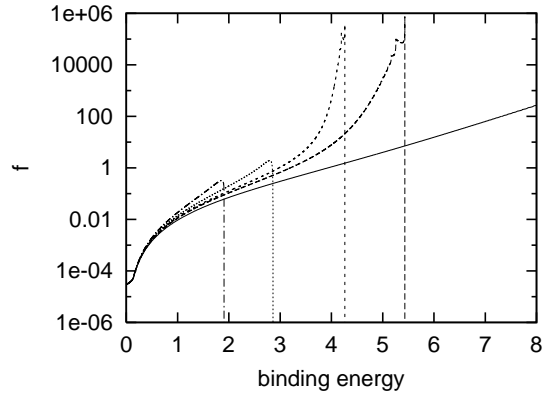


Fig. 8.— We show $f(\varepsilon)$ for various q ; Dot-dashed, dotted, short-dashed, dashed, and solid lines are for $q = 0.25, 0.5, 0.67, 0.75$, and 1.0 , respectively.

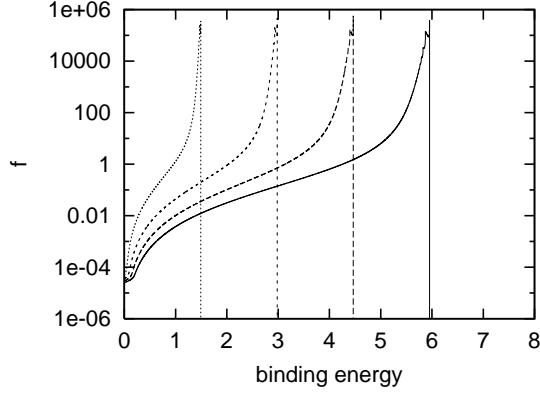


Fig. 9.— We show $f(\varepsilon)$ for various ε_0 ; Dotted, short-dashed, dashed, and solid lines are for $\varepsilon_0 = 0.5, 1.0, 1.5$, and 2.0 , respectively.

Table 1: The physical values of our simulated clusters

	Mass ($10^{15} M_{\odot}$)	T (10^8 K)	c
CLa	3.05	0.953	2.50
CLb	2.80	0.890	2.72
CLc ($z = 0$)	3.36	1.29	4.41
CLc ($z = 0.25$)	1.60	0.796	2.31
CLc ($z = 0.5$)	0.831	0.540	2.67
CLd	3.71	1.57	6.34
CLe	2.82	1.19	4.65
CLf	2.31	0.654	2.75

NOTE.— Each value is calculated at redshift $z = 0$, except for CLc.

Table 2: N_0 , q , and ε_0 of rich clusters in our numerical results

	N_0	q	ε_0
CLa	0.309	0.612	1.27
CLb	0.253	0.680	1.21
CLc ($z = 0$)	0.190	0.667	1.47
CLc ($z = 0.25$)	0.230	0.606	1.05
CLc ($z = 0.5$)	0.305	0.600	0.672
CLd	0.276	0.699	1.26
CLe	0.117	0.503	2.03
CLf	0.258	0.580	1.41

NOTE.— Each value is calculated at redshift $z = 0$, except for CLc.